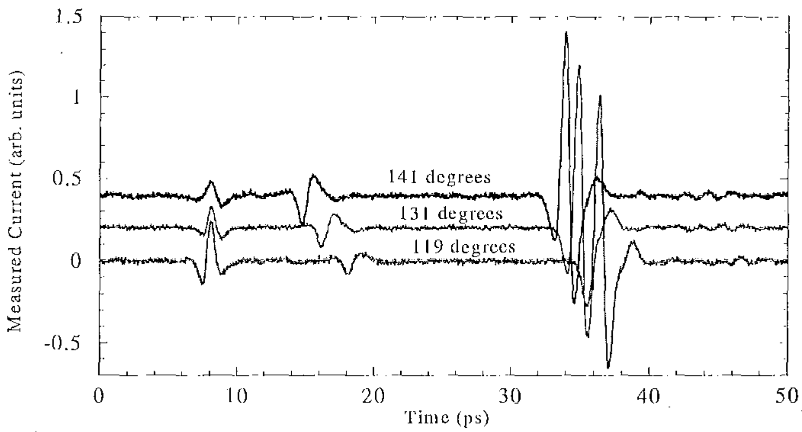

CThR1 **Fig. 2.** Impulse scattering measurement from an alumina cylinder over a range of bistatic angle from XXX to XXX degrees. The temporal and amplitude shifts of surface and transmitted waves are clearly visible.

1. D. Grischkowsky, "Nonlinear generation of sub-psec pulses of THz electromagnetic radiation by optoelectronics-applications to time domain spectroscopy," in *Frontiers in Nonlinear Optics*, H. Walther, N. Koroteev, M.O. Scully, eds. (Institute of Physics Publishing, Philadelphia, 1992).
2. R.W. McGowan, R.A. Cheville, D. Grischkowsky, "Experimental study of the surface waves on a dielectric cylinder via THz impulse ranging," IEEE Trans. Microwave Theory Tech., accepted for publication, 1999.
3. R.A. Cheville, R.W. McGowan, D. Grischkowsky, "Time resolved measurements which isolate the mechanisms responsible for terahertz glory scattering from dielectric spheres," Phys. Rev. Lett. **80,** 269–272 (1998).

CThR2 **3:00 pm**

Background-free THz imaging using interferometric tomography

J.L. Johnson, T. Dorney, D. Mittleman, *Department of Electrical and Computer Engineering, Rice Univ., Mailstop 366, 6100 Main St., Houston, Texas 77005, USA; E-mail: johnsojl@rice.edu*

THz imaging is an emerging technology that permits three-dimensional tomographic imaging of nonmetallic objects. Numerous applications have been demonstrated where THz imaging could be a valuable complement to existing technologies for noninvasive testing, including the detection of faults or delaminations in packaged integrated circuits and the location of air bubbles or cracks within polymer or ceramic parts.[1,2] In many of these applications, the feature one wishes to detect is subtle, in the sense that its interaction with the single-cycle THz pulse imposes only a small additional distortion on the waveform. A good example is the detection of a delamination or disbonding between two surfaces. In many practical cases, the gap which opens up between the two surfaces is narrower than the coherence length of the THz pulse, and the waveform is little changed as a result.

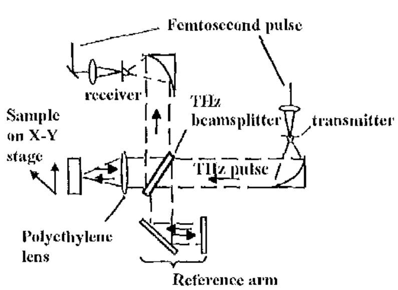

CThR2 **Fig. 1.** Schematic of terahertz T-ray imaging with interferometry.

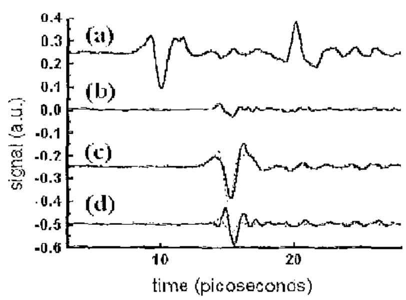

CThR2 **Fig. 2.** THz waveforms with (a) a delay between the signal and reference reflections, (b) the near cancellation of the two pulses, (c) the effect on the non-interferometric signal of 50-μm-thick adhesive tape, and (d) the effect on the interferometric signal of the tape.

Here we report on the use of interferometry in combination with THz tomography, for improving the detectability of such subtle features. This idea has analogies to optical coherence tomography, in which the signal pulse, reflected off of the sample, is interfered with a reference wave to provide enhanced sensitivity.[3] The experimental layout is shown in Fig. 1. The collimated THz beam is directed into a Michelson interferometer, in which one arm (signal) contains a 10-cm polyethylene lens. Thus, the THz beam is focused onto the sample at normal incidence. The second arm (reference) contains a planar mirror, mounted on a translation stage for variable delay. The measured signal is the coherent superposition of the electric fields from these two arms. Due to the Gouy phase shift acquired by the signal beam, it is 180° out of phase from the reference beam.[4] As a result, if the sample reflects the THz pulse without distortion, then the delay of the reference arm can be adjusted so that the two pulses destructively interfere at the detector, and almost no signal is detected. Figure 2(a) depicts a waveform in which the sample and reference pulses are separated in time by a few picoseconds. Figure 2(b) shows the waveform when the two pulses are overlapped in time, producing a near cancellation of the measured signal.

This cancellation relies sensitively on the delay and distortions acquired by the signal pulse when it interacts with the sample. Any small changes in this waveform produce large fractional changes in the measured signal. This is demonstrated using waveforms reflected off of a mirror with a piece of adhesive tape stuck on the surface. The thickness of this "defect" is approximately 50 microns, or 1/6 of the coherence length of the pulse.

CThR2 **Fig. 3.** Images comparing maximum peak-to-peak amplitude of (a) the normal, noninterferometric imaging and (b) interferometric imaging. The sample consists of two ~50-μm thick pieces of adhesive tape on a flat metal surface. In the upper image, only the edges of the two tape strips are faintly discernible. In the lower image, they are much more obvious; also, the tape strip on the right has two air bubbles, only discernible in the interferometric image. A median filter was used on both images.

The tape is composed of a transparent, low-index polymer, which has only a weak effect on the THz pulse. The waveforms shown in Figs. 2(c) and 2(d) represent comparisons between waveforms measured with and without the tape in the beam spot, for conventional [Fig. 2(c)] and interferometric [Fig. 2(d)] imaging. The contrast is evidently enhanced through the use of interferometry.

Figure 3 shows two images of the mirror with adhesive tape on its surface, with and without the use of interferometric imaging. The weak signal from the tape is substantially enhanced in the interferometric case [Fig. 3(b)], as is evident from these false-gray-scale images. In addition to the enhancement of contrast, the use of a background correction of this type can also suppress the effects of laser amplitude fluctuations or other noise sources. Finally, by canceling out the waveform reflected from a given surface, one can substantially enhance the detectability of a second nearby surface.

1. D. Mittleman, S. Hunsche, L. Boivin, M.C. Nuss, "T-ray tomography," Opt. Lett. 22(12), 904–906 (1997).
2. D. Mittleman, R.H. Jacobsen, M.C. Nuss, "T-ray imaging," IEEE J. Sel. Top. Quant. Elec. 2(3), 679–692 (1996).
3. D. Huang, E. Swanson, C. Lin, J. Schuman, W. Stinson, W. Chang, M. Hee, T. Flotte, K. Gregory, C. Puliafito, J. Fujimoto, "Optical coherence tomography," Science 254, 1178–1181 (1991).
4. A.B. Ruffin, J.V. Rudd, J.F. Whitaker, S. Feng, H.G. Winful, "Direct observation of the Gouy phase shift with single-cycle terahertz pulses," Phys. Rev. Lett. 83(17), 3410–3413 (1999).

CThR3 **3:15 pm**

Electro-optic-based two-dimensional THz near-field imaging

Q. Chen, Z. Jiang, X.-C. Zhang, *Department of Physics, Applied Physics, and Astronomy, Rensselaer Polytechnic Inst., Troy, New York, 12180, USA; E-mail: zhangxc@rpi.edu*

Since the first demonstration of THz imaging by Hu and Nuss,[1] many different approaches have been proposed to improve its spatial resolution, the data acquisition time and extend its application, such as T-Ray tomography,[2] THz near-field imaging,[3] and real-time two-dimensional (2D) THz electro-optic imaging.[4,5] Among them, the last one shows a unique advantage on the data acquisition rate, which is only limited by the CCD camera. With our newly developed dynamic subtraction technique with the frame rate as high as 70 frames per second, the signal-to-noise ratio was improved by about two orders. But the system spatial resolution of the usual 2f-2f 2D imaging system is basically limited by aberration and diffraction of THz beam, because the electro-optic (EO) sensor is positioned at the conjugate plane of the object, which corresponds to the far-field of the THz beam.

THz near-field measurement is an effective way to improve the spatial resolution of imaging system. It is obviously not possible to realize near-field imaging in the conventional transmission EO sampling geometry because the object put right in front of the sensor will block the probe beam. Therefore we change to the reflection geometry. As shown in Fig. 1, the incidence of THz beam is on the front surface of the EO crystal, whereas that of probe beam is on the back surface. The probe beam will be reflected by the front surface of the EO crystal and collinearly propagates with the THz beam in the sensor. It has been proved experimentally as well as theoretically that the THz waveform measured in this reflection geometry is the same as that in the transmission geometry. The reason is that the EO signal from the counter-propagating THz beam and probe beam is negligible. The object can then be located right in front of the EO crystal, and realize the near-field measurement of THz field.

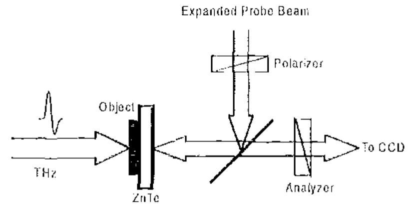

CThR3 Fig. 1. Schematic illustration of the real-time 2D THz near-field imaging system.

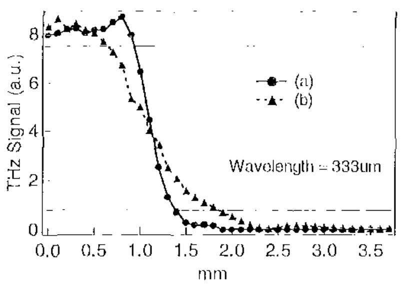

CThR3 Fig. 2. The scan of a razor blade through the THz beam. (a) Razor blade scans through the THz near field. (b) Razor blade scans through the THz focal point.

We first test the improvement of the spatial resolution by applying the above reflection geometry in the conventional scanning THz imaging setup. To measure the near-field THz beam size, a razor blade, which was almost in contact with the ZnTe sensor in the above EO sampling geometry, was scanned through the THz beam. The same measurement was also carried out by scanning the razor blade through the THz focal point in the conventional scanning imaging system. In this case, the measured THz beam size will be larger, which is due to the diffraction effect. The result is shown in Fig. 2. From the distance between the 90% and the 10% of maximum signal level, we can quantify the spatial resolution for the near-field measurement as 0.4 mm (curve a) and 1.2 mm for the THz focal point (curve b). We see the spatial resolution was improved by three times and the resolution in near-field geometry is close to the related wavelength.

It should be emphasized that the above result is from the scanning imaging system with the focused THz and probe beams on the EO sensor and single detector. In principle, the spatial resolution of the scanning imaging system and CCD imaging system would have similar spatial resolution if similar THz sources and system numerical apertures were used. However, by taking the aberration and the difference on SNR into consideration, the scanning system generally has better spatial resolution. Compared with the conventional 2f-2f 2D imaging system, the spatial resolution of near-field imaging setup (Fig. 1) can improve more as shown by following experimental results. We imaged a metal word "THz" by positioning it right in front of the ZnTe sensor in the above near-field setup. The image can be displayed on the computer monitor in real time (Fig. 3), which is the unique capability of the CCD imaging system. The metal letters are formed by metal line with a width of 0.5 mm, the size of the word is 1 cm × 0.5 cm. We can thus estimate that the system spatial resolution is at least 0.5 mm, which can not be realized in the conventional 2f-2f imaging system. In the above experiment, a larger aperture antenna was used as THz emitter, whose peak frequency is 0.3 THz. If such an emitter were used in the 2f-2f imaging system with 0.5 system numerical aperture, the best system spatial resolution could be estimated as about 2.5 mm in paraxial condition. Considering the system aberration, we can reasonably conclude that the spatial resolution is improved by about one order in this near-field CCD imaging setup (compared with the 2f-2f imaging system). The above result also shows the capability to image moving and life objects by such a system.

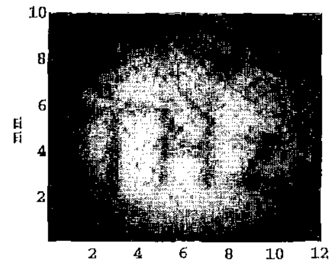

CThR3 Fig. 3. Real-time 2D THz near-field imaging of a metal word "THz."

1. B.B. Hu, M.C. Nuss, Opt. Lett. 20, 1716 (1995).
2. D. Mittleman, S. Hunsche, L. Boivin, M.C. Nuss, Opt. Lett. 22, 904 (1997).
3. S. Hunsche, M. Koch, I. Breuer, M.C. Nuss, Opt. Commun. 150, 22 (1998).
4. Q. Wu, T.D. Hewitt, X.-C. Zhang, Appl. Phys. Lett. 69, 1026 (1996).
5. Z.G. Lu, P. Campbell, X.-C. Zhang, Appl. Phys. Lett. 71, 593 (1997).

CThR4 **3:30 pm**

Dielectric terahertz waveguides

S.P. Jamison, R.W. McGowan, D. Grischkowsky, *School of Electrical and Computer Engineering and Ctr. for Laser and Photonic Res., Oklahoma State Univ., Stillwater, Oklahoma 74078, USA; E-mail: danielg@thzsun.ecen.okstate.edu*

We believe we report the first demonstration of waveguide propagation of sub-ps THz

Thursday, May 11